

Polymerized High Internal-Phase Emulsions: Properties and Interaction with Water

ANATOLY Y. SERGIENKO,¹ HUIWEN TAI,¹ MOSHE NARKIS,² MICHAEL S. SILVERSTEIN¹

¹ Department of Materials Engineering, Technion–Israel Institute of Technology, Haifa, 32000, Israel

² Department of Chemical Engineering, Technion–Israel Institute of Technology, Haifa, 32000, Israel

Received 26 June 2001; accepted 15 August 2001

ABSTRACT: The synthesis and characterization of novel polymerized high internal-phase emulsions (polyHIPE) materials are described. Homogeneous, highly porous, low-density, open-cell crosslinked copolymers were prepared by polymerizing the continuous phase of HIPE containing styrene and varying amounts of 2-ethylhexyl methacrylate. The glass transition temperatures (T_g s) of the homopolymers were similar to the literature values, but the copolymer T_g s were lower than expected. These results indicate that the copolymer composition is richer in 2-ethylhexyl methacrylate than the feed composition. The homopolymer moduli, calculated from the foam moduli, were similar to the literature values. The influence of composition and surface treatment on the water absorbed by the foams was investigated. For example, washing a polyHIPE based on poly(ethylhexyl acrylate) in water at 70°C increased water absorption because of the removal of the residual salt. Adding a fluorinated comonomer to the HIPE reduced hydrophilicity and, thus, water absorption. © 2002 Wiley Periodicals, Inc. *J Appl Polym Sci* 84: 2018–2027, 2002; DOI 10.1002/app.10555

Key words: high internal-phase emulsion (HIPE); water absorption; polystyrene; poly(ethylhexyl acrylate); poly(ethylhexyl methacrylate)

INTRODUCTION

A high internal-phase emulsion (HIPE) is defined as an emulsion in which the dispersed phase occupies more than 74% of the volume, the maximum packing fraction of monodispersed spheres. The continuous phase, which generally constitutes less than 26% of the final volume, can contain monomers and crosslinking comonomers. A polyHIPE is a microporous material produced by the polymerization of the monomers in the con-

tinuous phase of a HIPE.^{1–3} Microporous foams of very high void fractions (porosities of up to 97%) can be made through polyHIPE synthesis.⁴ The monomers and an organic soluble surfactant form the continuous organic phase; water containing a water-soluble initiator (potassium persulfate) and a stabilizer (potassium sulfate or calcium chloride) forms the dispersed aqueous phase. Investigations into the factors that affect the cellular structure and morphology of poly(styrene/divinylbenzene) [P(S/DVB)] polyHIPE revealed that the surfactant concentration plays a pivotal role.⁵ Cryo-SEM studies⁶ have shown that the appearance of holes between adjacent water droplets correspond to the gel point of the polymerization. The cell sizes of P(S/DVB) polyHIPEs were found to be strongly affected by the concentration

Correspondence to: M. S. Silverstein (michaels@tx.technion.ac.il).

Contract grant sponsors: Water Research Institute; Technion VPR Fund.

Journal of Applied Polymer Science, Vol. 84, 2018–2027 (2002)
© 2002 Wiley Periodicals, Inc.

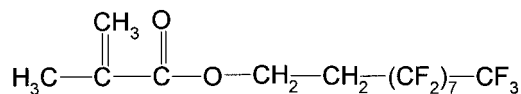


Figure 1 Scheme for perfluorooctylethyl methacrylate (FMA).

of electrolytes in the aqueous phase⁷; increasing the salt concentration tended to lower the cell size. The presence of salt is known to enhance water-in-oil emulsion stability via inhibition of the Ostwald ripening process, by reducing the miscibility of the organic and aqueous phases.⁸ Additionally, electrolytes lower the interfacial tension, thus yielding greater surfactant adsorption at the interface and increasing the resistance to droplet coalescence.⁹

Open-cell polyHIPEs are characterized by a low bulk density, typically less than 0.15 g/cm³, and cell sizes that range between 5 and 100 μm, depending on the preparation conditions. Consequently, the internal surface areas tend to be much lower than observed in typical P(S/DVB) bead resins, 5 m²/g being an average figure. PolyHIPEs with surface areas up to 350 m²/g can be prepared by using porogens in the organic phase,¹⁰ in which the cell walls have pores similar in size and character to those observed in conventional macroporous polymer resins.¹¹

PolyHIPEs possess many unique properties resulting from their highly porous, open-cell structure and low density. Polystyrene polyHIPE foams have higher compressive strengths than conventional gas-blown polystyrene foams.⁵ PolyHIPE are able to rapidly absorb large quantities of liquid through capillary action.¹ The simple immersion of a piece of the polyHIPE in a liquid yields rapid absorption within the pores, accompanied by the displacement of air. The surface tension, solubility parameter, and viscosity of the liquid will affect the capillary driving force and thus the volume which will be absorbed.¹⁰ Methanol, which is a nonswelling solvent for crosslinked polystyrene, is absorbed in the pores while toluene is absorbed both in the pores and in the polystyrene, causing the walls of the foam to swell. The absorption of very polar liquids such as water may be quite low, reflecting polymer hydrophobicity.¹⁰

The preparation, properties, and applications of polyHIPE polymers have been reviewed.¹² PolyHIPE materials have been successfully employed as supports in solid-phase peptide synthesis, with the porous structure acting as a scaffold

for a soft polyamide gel.¹³ Additionally, polyHIPE monoliths were used to immobilize flavin,¹⁴ and granulated P(S/DVB) polyHIPE was used as a catalyst support.¹⁵ PolyHIPE copolymers containing styrene (S) and varying amounts of either 2-ethylhexyl acrylate (EHA) or 2-ethylhexyl methacrylate (EHMA) were also investigated.¹⁶

Previous work focused on polyHIPE interpenetrating polymer networks¹⁷ and polyHIPE organic/inorganic hybrids.¹⁸ In the present study, polyHIPE were synthesized by using various monomers including S, EHA, EHMA, and perfluorooctylethyl methacrylate (FMA). All the polyHIPEs were crosslinked by using DVB as a comonomer. The morphology, thermal properties, mechanical properties, and water absorption of the polyHIPE were investigated.

EXPERIMENTAL

Materials

The monomers used for polyHIPE synthesis were S (purity > 99%, Fluka Chemie), DVB (which contains 40% ethylstyrene, Riedel-de-Haen), EHA (purity > 98%, Aldrich Chemical Co.), EHMA (purity > 98%, Aldrich Chemical Co.), and FMA (Clariant). The structure of FMA is illustrated in Figure 1. The monomers were used as received. The emulsifiers, whose structures are illustrated in Figure 2, were sorbitan monooleate (SMO, Span 80, Fluka Chemie) and sorbitan monolaurate (SML, Span 20, Fluka Chemie). The water-soluble initiator was potassium persulfate

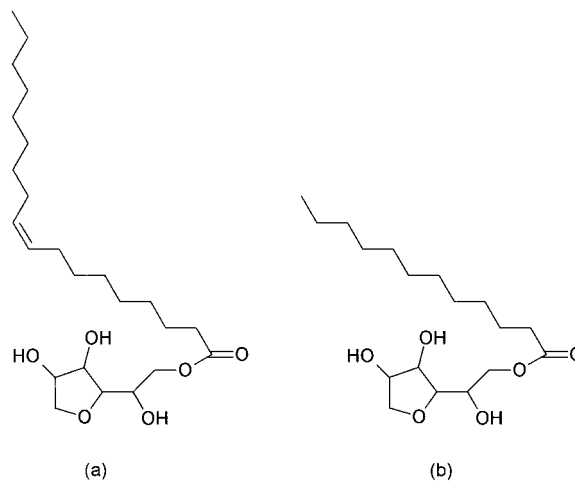


Figure 2 Schemes for the emulsifiers: (a) SMO; (b) SML.

Table I Recipe for P(S/EHMA/DVB)-45/45/10 PolyHIPE

Organic phase (g)	Styrene	4.5
	EHMA	4.5
	DVB	1
	SMO	2
Aqueous phase (g)	H ₂ O	90
	K ₂ S ₂ O ₈	0.2
	K ₂ SO ₄	0.5

(K₂S₂O₈, purity > 99%, Riedel-de-Haen). The HIPE stabilizers were potassium sulfate (K₂SO₄, chemical pure, Frutarom, Haifa, Israel) and calcium chloride hydrate (CaCl₂·2H₂O, chemical pure, BDH Chemicals Ltd., Dorset, England).

PolyHIPE Synthesis

The HIPE emulsion was formed by adding the aqueous phase (water, initiator, and stabilizers, about 90% of the total volume) drop-wise to the organic phase (monomers and emulsifier, about 10% of the total volume). The recipe for preparing a P(S/EHMA/DVB)-45/45/10 polyHIPE is listed in Table I. SMO, with a hydrophilic/lipophilic balance (HLB) of 4.3, was the emulsifier used for P(S/DVB) and P(S/EHMA/DVB). SML, with a HLB of 8.6, was the emulsifier used for P(EHA/DVB) and P(EHMA/DVB/FMA). The choice of emulsifier for a particular monomer was based on the stability of the HIPE formed (the less stable HIPE begins to separate into two phases). An equal amount of surfactant (20 wt % of organic phase) was used for the preparation of all the polyHIPEs. The amount of DVB used for preparing all the P(S/EHMA/DVB) polyHIPEs was 10 wt %. PolyHIPEs with EHA contained at least 20%

DVB because a smaller DVB content yielded significant polyHIPE shrinkage during drying. The various polyHIPEs studied are listed in Table II.

The detailed procedure for preparing P(S/EHMA/DVB)-45/45/10 was as follows: the organic phase was placed in a 250-mL beaker and stirred with a magnetic stirring bar. The aqueous phase was added drop-wise, with constant stirring. The stirring continued for an additional 5 min after all the aqueous phase had been added. The resulting HIPE was covered with Saran Wrap[®] and placed in an oven at 65°C for 18 h for polymerization. The resulting polyHIPE was removed from the beaker. The water was removed from the polyHIPE by drying in a vacuum oven at 60°C for about 2 days until a constant weight was achieved. The drying was generally relatively rapid, reflecting the open-cell structure of the foam.

Extraction

The surfactant and salt, which remained in the polyHIPE following drying, were removed (when needed) by extraction. The polyHIPE was placed in a Soxhlet apparatus and extracted with water and then with methanol for 24 h each and dried in a convection oven at 60°C for 12 h.

PolyHIPE Modification

The polyHIPEs were modified in an attempt to enhance hydrophilicity and, thus, water absorption. Two methods were used in an attempt to increase the hydrophilicity of poly(ethylhexyl acrylate) (PEHA) polyHIPEs: (1) PEHA was placed in water at 70°C and dried in a convection oven at 60°C for 12 h; (2) PEHA was immersed in a beaker containing a 20 vol % aque-

Table II PolyHIPE Yield and Density

PolyHIPE	Y_a	Y_b	R_m	Density (g/cm ³)
P(S/DVB)-90/10	0.71	0.70	1.0	0.12
P(EHMA/S/DVB)-22.5/67.5/10	0.74	—	—	0.10
P(EHMA/S/DVB)-45/45/10	0.70	0.72	1.0	0.11
P(EHMA/S/DVB)-65/25/10	0.99	—	—	0.12
P(EHMA/DVB)-90/10	0.97	0.96	1.0	0.14
P(EHA/DVB)-80/20	0.98	0.99	1.0	0.11
P(EHA/DVB)-70/30	1.00	—	—	0.12
P(EHA/DVB)-60/40	1.00	—	—	0.11
P(EHMA/DVB/FMA)-5/3/2	0.90	—	—	0.12
P(EHMA/DVB/FMA)-6/3/1	0.84	—	—	0.12

ous solution of acrylic acid and 0.05 wt % potassium persulfate at room temperature for 30 min. The beaker was then placed in an oven at 60°C for 30 min for acrylic acid polymerization. The foam was removed from the beaker and dried in a convection oven at 60°C for 12 h.

Structure and Property Characterization

The cell structure was studied by using high-resolution scanning electron microscopy of polyHIPE cryogenic fracture surfaces (HRSEM, Zeiss LEO 982). The samples, viewed by using accelerating voltages from 1 to 3 kV, were not coated. The foam density was determined by measuring the mass and volume of a specimen.

The thermal properties (glass transition temperature, T_g) of the foams were investigated by using a dynamic mechanical thermal analysis temperature sweep (DMTA, Rheometrics MKIII). Samples, $5 \times 5 \times 5 \text{ mm}^3$, were subjected to a sinusoidal compressive strain at a frequency of 1 Hz while heated at a rate of 3°C/min. The T_g s were taken from the E'' peak. The compressive moduli of the polyHIPEs were determined from the initial slope of compressive stress–strain curves at room temperature (Rheometrics MKIII). Samples, $5 \times 5 \times 5 \text{ mm}^3$, were subjected to a compressive force at a rate varying from 0.0167 to 0.0233 N/s for PEHMA and PS polyHIPEs, respectively. The modulus is an average of two samples (the variation was $\pm 9\%$).

Fourier transform infrared (FTIR) spectra were collected from the polyHIPE without any sample preparation (Bruker Equinox 55 FTIR using a photoacoustic accessory).

The water absorption within the cells of the polyHIPE was studied as a function of time. The samples were weighed, placed on the surface of the water in a beaker and weighed, without blotting, every minute for the first 10 min and at longer intervals during the following hour. During the experiment, the samples floated on the surface of the water. The amount of weight gain (WG) was calculated by using

$$WG = [(m_{\text{wet}} - m_{\text{dry}})/m_{\text{dry}}]100\% \quad (1)$$

where m_{dry} is the mass of the dry polyHIPE specimen, before experiment, and m_{wet} is the mass of the polyHIPE with imbibed water.

RESULTS AND DISCUSSION

PolyHIPE Yield and Density

The yields of the polyHIPE (Table II) were calculated assuming that all the surfactant and salt remain within the polyHIPE:

$$Y_a = (m_f - m_{\text{srf}} - m_{\text{slt}})/m_m \quad (2)$$

where m_f is the final weight of polyHIPE after drying, m_{srf} is the weight of the surfactant used, m_{slt} is the weight of the stabilizing salt used, and m_m is the weight of the monomers used. This assumption was verified for several polyHIPEs by calculating the yield following extraction (Table II) by using

$$Y_b = m_{\text{ext}}/m_m \quad (3)$$

where m_{ext} is the weight of polyHIPE after a Soxhlet extraction with water and then with methanol for 24 h each. The ratio of the mass extracted from the polyHIPE to the total salt and surfactant used, R_m (4), is approximately 1, verifying the validity of eq. 2 and the assumptions that the surfactant and salt remain in the polyHIPE but can be removed through extraction;

$$R_m = (m_f - m_{\text{ext}})/(m_{\text{srf}} + m_{\text{slt}}) \quad (4)$$

The yield varies from 0.70 to 0.74 when S is present as a comonomer. These relatively low yields were caused by the inhibitor that was not removed from S prior to the polymerization. When the inhibitor was removed by washing with 5 wt % NaOH aqueous solution, the yield for P(S/DVB) polyHIPE reached 0.81. The acrylic monomers exhibited yields of 0.84 to 1.

The densities of the polyHIPEs in Table II varied from a minimum 0.10 g/cm³ for P(EHMA/S/DVB)-22.5/67.5/10 to a maximum of 0.14 g/cm³ for P(EHMA/DVB)-90/10. There was no apparent relationship between the density and the comonomer composition.

Cell Structure

The polyHIPEs have an open-cell morphology with cells, cell walls, and intercellular pores within the cell walls, as seen in the SEM micrographs in Figure 3. P(S/DVB) [Fig. 3(a)] has cells 3–10 μm in diameter and intercellular pores 0.4–1.5 μm in diameter. P(EHMA/DVB) [Fig. 3(b)] has

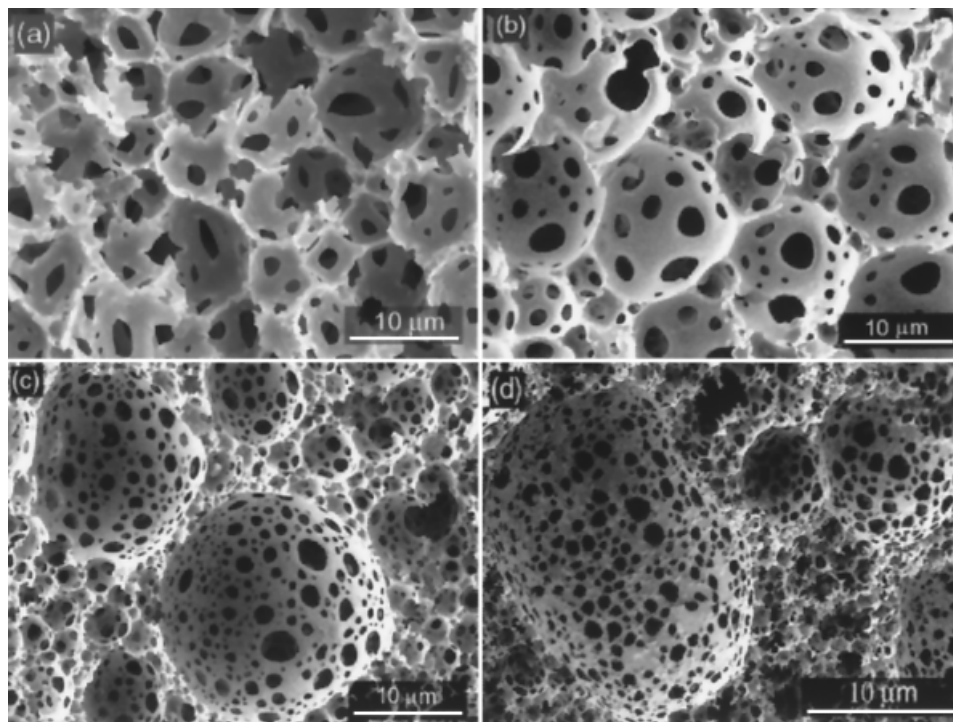


Figure 3 SEM micrographs of polyHIPE cryogenic fracture surfaces: (a) P(S/DVB)-90/10; (b) P(EHMA/DVB)-90/10; (c) P(EHA/DVB)-80/20; (d) P(EHMA/DVB/FMA)-50/30/20.

cell and intercellular pore sizes that are similar to those of P(S/DVB). The pores for P(S/DVB) are ellipsoidal, bordering on trapezoidal, with angular cusps instead of rounded corners. On the other hand, the pores for P(EHMA/DVB) and P(EHA/DVB) in Figure 3(b,c), respectively, are more circular in shape. P(EHA/DVB) and P(EHMA/DVB/FMA) in Figure 3(c,d), respectively, exhibit a significantly wider, almost bimodal, distribution of cell diameters. The average diameter of the smaller cells is $1.5 \mu\text{m}$ and the average diameter of the larger cells is $15 \mu\text{m}$ for both foams. These foams also have relatively high densities of intercellular pores and relatively small pore diameters, ranging from 0.3 to $1 \mu\text{m}$.

These differences in cell size, cell-size distribution, intercellular pore size, and intercellular pore density most likely result from the use of a different surfactant for the P(EHA/DVB) and P(EHMA/DVB/FMA) foams. SML, a surfactant with a higher HLB balance, was used for P(EHA/DVB) and P(EHMA/DVB/FMA), whereas SMO was used for P(EHMA/DVB), P(S/DVB), and their copolymers.

As the water-to-monomer ratio reaches 5/1, the viscosities of the HIPE prepared by using SML

were significantly higher than those prepared by using SMO. This higher HIPE viscosity is related to SML's higher HLB and its higher viscosity. The smaller cells in the bimodal cell-size distribution with SML may reflect the small droplets formed in the early stages of HIPE synthesis. In the early stages, at low water-to-monomer ratios, the shear stress of mixing in the low viscosity system is able to break up any large droplets. Larger cells are formed at higher water-to-oil ratios when the system is more viscous and the shear stress of mixing is unable to break up any large droplets and unable to produce a homogeneous droplet size distribution. The viscosity remained low throughout HIPE formation with the more hydrophobic SMO and, therefore, stirring the low viscosity system yielded a homogeneous droplet distribution. The differences in interfacial tension between the two systems also contributed to the differences in cell size and size distribution. Despite these differences in cell structure, the densities of the foams were similar.

Thermal and Mechanical Properties

A DMTA temperature sweep typical for these foams is seen for P(S/DVB)-90/10 in Figure 4. The

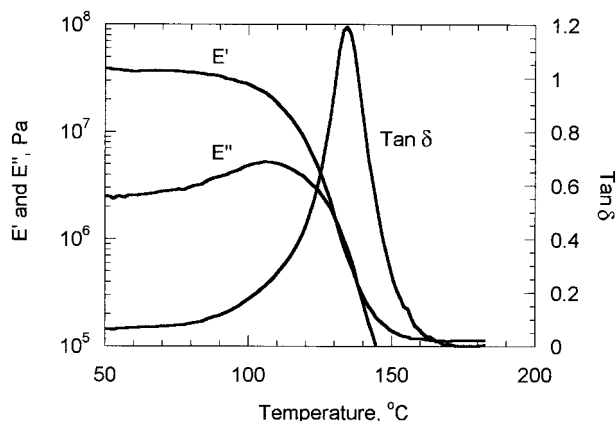


Figure 4 DMTA temperature sweep for P(S/DVB)-90/10.

T_g s of P(S/DVB) and P(EHMA/DVB), 106 and -8°C , respectively, were taken from the E'' peak and are in close agreement with the literature values.¹⁹

The effects of DVB content on P(EHA/DVB) E' and E'' are seen in Figures 5 and 6, respectively. There is a distinct increase in E' at high temperatures (above the T_g) with increasing DVB content, reflecting the increased crosslink density (Fig. 5). The height of the E'' peak decreases with increasing DVB content (Fig. 6). This decrease in E'' reflects a reduction in the damping exhibited by foams stiffened by higher crosslink densities. The E'' peaks shift to higher temperatures with increasing DVB content, as expected from the higher inherent stiffness of DVB as well as from the increase in crosslink density. The T_g increases from -40°C for P(EHA/DVB)-80/20 to -29 and -23°C for P(EHA/DVB)-70/30 and P(EHA/DVB)-

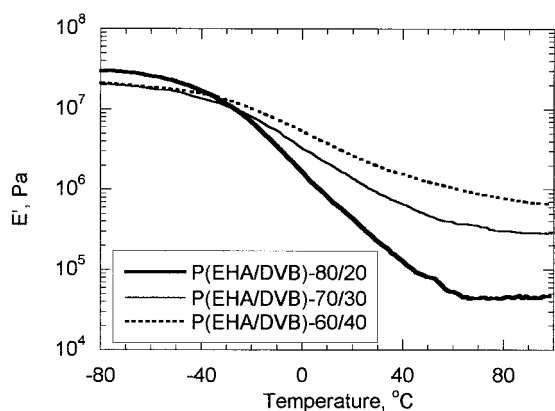


Figure 5 Variation of E' with temperature for P(EHA/DVB) with various amounts of DVB.

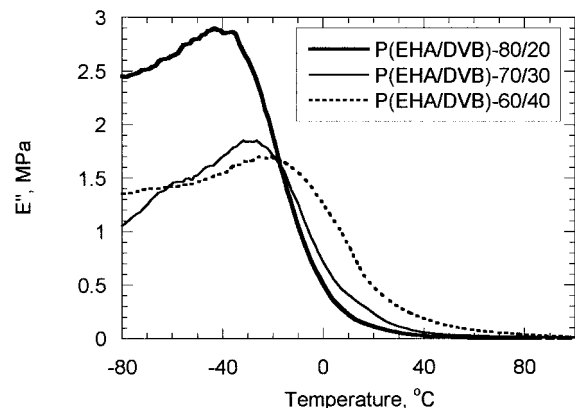


Figure 6 Variation of E'' with temperature for P(EHA/DVB) with various amounts of DVB.

60/40, respectively. The variation of T_g with DVB content is seen in Figure 7.

The variation in T_g with S content in P(S/EHMA/DVB) polyHIPE is seen in Figure 8. The experimental results are presented as well as the arithmetic average and the T_g predicted by the Fox equation²⁰:

$$\frac{1}{T_g} = \sum_i \frac{w_i}{T_{gi}} \quad (5)$$

where w_i is the weight fraction of comonomer i and T_{gi} is the T_g of the homopolymer from monomer i ($i = 1, 2$). In this case, the homopolymer T_g s were the experimental results for the P(S/DVB) and P(EHMA/DVB) polyHIPE. The T_g increases with S content, as expected. The relatively low T_g s at low S contents seem to indicate that the EHMA content in the polymer is higher than that

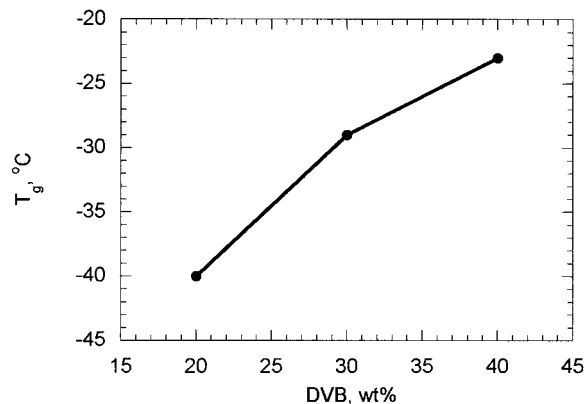


Figure 7 Variation of P(EHA/DVB) T_g with DVB content.

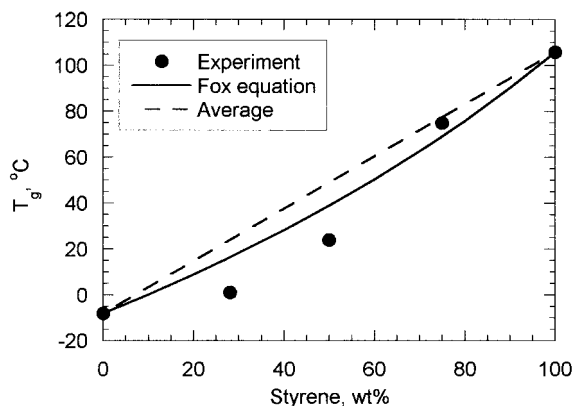


Figure 8 Variation of P(S-co-EHMA/DVB) T_g with styrene content.

in the feed. The lower yield for the P(S/DVB) synthesis compared to the P(EHMA/DVB) synthesis (Table II) reflects the lower reactivity of the S. Thus, the lower reactivity of S yields a lower S content in P(S/EHMA/DVB) than would be expected from the feed composition and this is reflected in a lower T_g than expected.

Room-temperature compressive stress–strain curves for various P(S/EHMA/DVB) copolymers are seen in Figure 9. The foams with S/EHMA ratios of one or less behave similar to P(EHMA/DVB). These foams exhibit a linear stress–strain region, from which the foam modulus is derived, a plateau region, and a densification region, all typical of foam compressive stress–strain behavior. The stress–strain curves for foams with S/EHMA ratios of 3/1 and greater were halted within the plateau region (brittle crushing) owing to an experimental limitation on the compressive force. The foams with S/EHMA ratios of 3/1 and greater

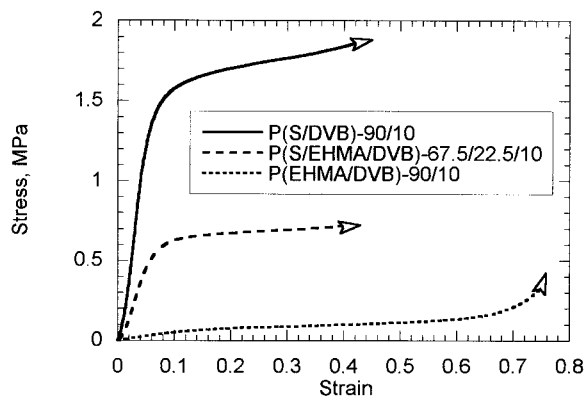


Figure 9 Compressive stress–strain curves for various foams.

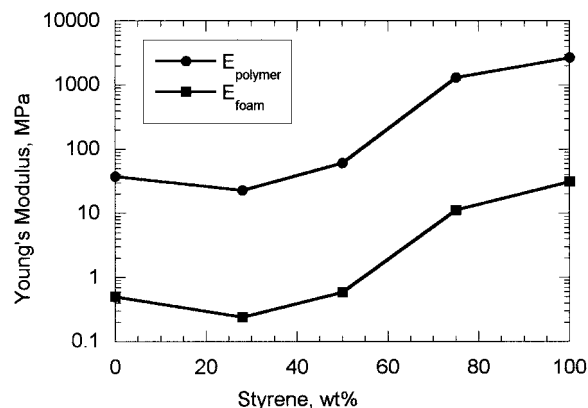


Figure 10 Variation of foam and polymer compressive moduli with S content for P(S-co-EHMA/DVB)-90/10 copolymers.

had higher moduli and thus reached the experimental limit on force at lower strains.

The variation of polyHIPE and polymer moduli with S content for the P(S/EHMA/DVB) copolymers is seen in Figure 10. The polyHIPE modulus (E_{foam}) is the initial slope from the stress–strain curve. The modulus of the polymer (100% dense) (E_{polymer}) was calculated by using²¹

$$E_{\text{polymer}} = E_{\text{foam}}(\rho_{\text{polymer}}/\rho_{\text{foam}})^2 \quad (6)$$

where ρ_{foam} is the polyHIPE density and ρ_{polymer} is the bulk polymer density. The densities of PS and PEHMA were taken as 1.05 and 1.2 g/mL, respectively.²² The density of the copolymers was calculated by using

$$\frac{1}{\rho_{\text{polymer}}} = \sum_i \frac{w_i}{\rho_i} \quad (7)$$

where w_i is the mass fraction of polymer i ($i = 1, 2$). The resulting polymer moduli of 2.7 GPa for PS and 38 MPa for PEHMA are in good agreement with the literature values.²² Here again, the EHMA content in the polymer is greater than that in the feed, yielding lower than expected moduli for EHMA/S of 65/25 and 45/45.

Water Absorption

The variation of water absorption (in percentage of polyHIPE sample weight) with time for various foams is seen in Figure 11. There is a rapid increase in water absorption during the first 15

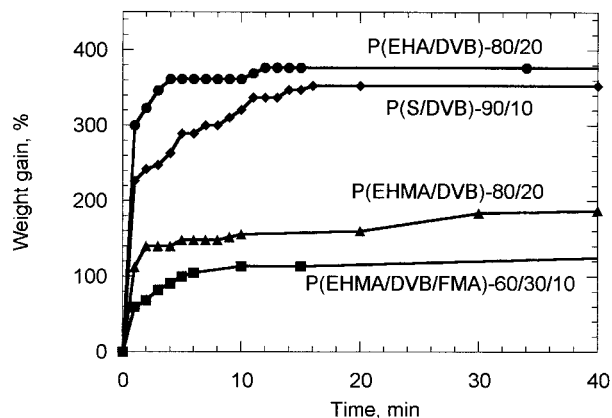


Figure 11 Water absorption as a function of time for various foams.

min, after which a plateau is reached. P(EHA/DVB) attains the highest water absorption, a plateau of 378%. The foam containing a fluorocarbon comonomer [P(EHMA/DVB/FMA)] exhibits an extremely low water absorption value (97%). This low absorption reflects the hydrophobicity of the polymer with the fluorine-rich comonomer.

An unexpectedly significant reduction in water absorption, as seen in Figure 12, resulted in modifying P(EHA/DVB) with poly(acrylic acid). Coating the surface with poly(acrylic acid) was expected to enhance hydrophilicity and, thus, enhance water absorption. The explanation for these results is found in the changes in the cell structure. The structure of unmodified P(EHA/DVB) [Fig. 3(c)] can be compared to the structure following polymerization of acrylic acid within the foam (Fig. 13). Poly(acrylic acid) did not coat the walls, but, rather filled the cells, closing the open-cell structure and reducing porosity. Thus, the

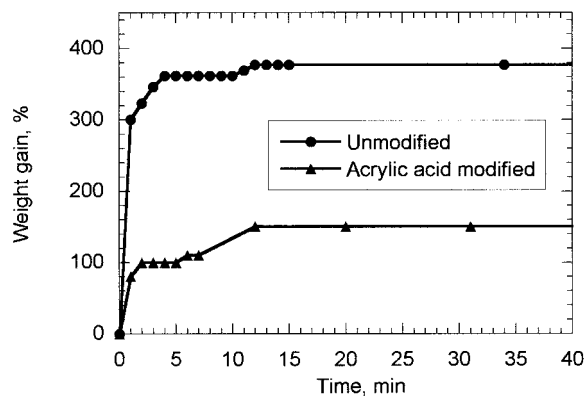


Figure 12 Water absorption as a function of time for P(EHA/DVB)-80/20: unmodified; acrylic acid modified.

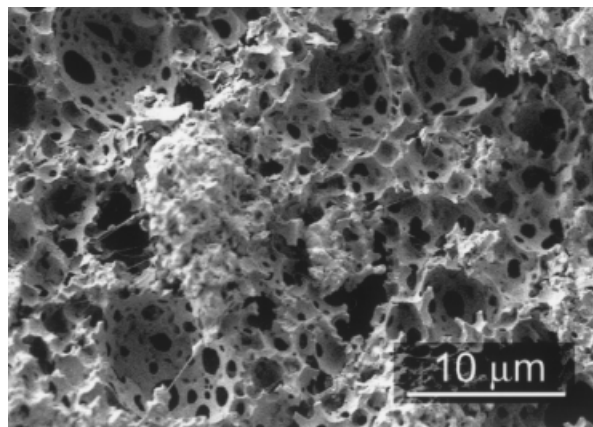


Figure 13 SEM micrograph of acrylic acid modified P(EHA/DVB)-80/20 cryogenic fracture surface.

poly(acrylic acid) treatment disrupted the open-cell structure and prevented water from penetrating the foam.

There was a significant enhancement in P(EHA/DVB) water absorption following washing in water at 70°C for 3 h (Fig. 14). The water absorption increases from 350% for P(EHA/DVB) to 506% following washing. The changes in the polyHIPE upon washing can be characterized by using FTIR. The FTIR spectra of EHA, SML, and $\text{CaCl}_2 \cdot 2\text{H}_2\text{O}$ are presented in Figure 15. Both SML and $\text{CaCl}_2 \cdot 2\text{H}_2\text{O}$ have significant $-\text{OH}$ peaks at 3400 cm^{-1} . $\text{CaCl}_2 \cdot 2\text{H}_2\text{O}$ has a peak related to water at 1632 cm^{-1} .²³ The FTIR spectra for P(EHA/DVB)-80/20 polyHIPE before washing, after washing, and after Soxhlet extraction in methanol are presented in Figure 16. After washing, the peak at 1632 cm^{-1} disappeared, indicating that

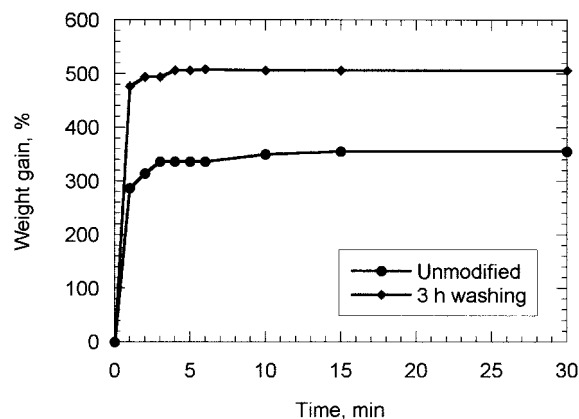


Figure 14 Water absorption as a function of time for P(EHA/DVB)-80/20 polyHIPEs: unmodified; washed with water at 70°C for 3 h.

the salt, present in the as-synthesized polyHIPE, was removed. The FTIR spectrum of a P(EHA/DVB) polyHIPE synthesized without $\text{CaCl}_2 \cdot 2\text{H}_2\text{O}$ is identical to Figure 16(b). There is no $-\text{OH}$ peak in the neighborhood of 3400 cm^{-1} following Soxhlet extraction in methanol, indicating that the surfactant was removed. These results confirm that the surfactant and salt remain in the polyHIPE.

CONCLUSION

A series of copolymer foams was prepared from high internal-phase emulsions. The foams had an open-cell structure with cells ranging from 1.5 to $15\ \mu\text{m}$ in diameter, intercellular pores ranging from 0.3 to $1.5\ \mu\text{m}$ in diameter, and densities ranging between 0.10 and $0.14\ \text{g/cm}^3$. The emulsifier had a dominant effect on the cell size and size distribution. SML produced numerous small cells through a reduction of interfacial tension and several large cells owing to the increase in viscosity at high water-to-oil ratios. SMO produced a uniform cell size because of the lower viscosity of the resulting HIPE. Both the salt and the surfactant remain in the polyHIPE following synthesis.

The T_g of PEHA and PS were -8 and 106°C , respectively, and the compressive moduli of the polymers were 38 MPa and 2.7 GPa, respectively, consistent with the literature values. The relatively low yield for S yielded copolymers with lower S contents than the feed and thus copolymer T_g s and moduli which were lower than expected.

The PS and PEHA foams absorbed over 350% of their weight in water. Washing the PEHA polyHIPE in water at 70°C removed the salt from the

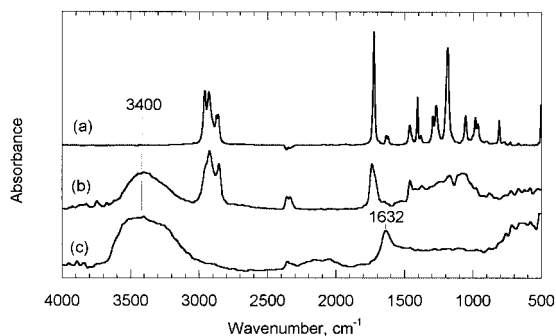


Figure 15 FTIR spectra of (a) EHA; (b) SML; (c) $\text{CaCl}_2 \cdot 2\text{H}_2\text{O}$.

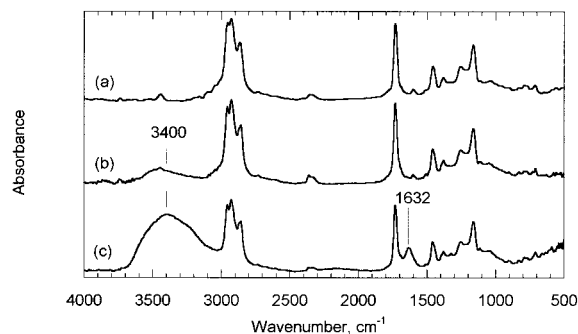


Figure 16 FTIR spectra of P(EHA/DVB)-80/20 polyHIPEs: (a) Soxhlet extracted with water and methanol; (b) washed with water at 70°C for 3 h; (c) unmodified.

polyHIPE and increased the water absorption to 500%. Soxhlet extraction with methanol removed the surfactant from the polyHIPE. Copolymerization with a fluorinated monomer reduced hydrophilicity and, therefore, the water absorption.

The partial support of the Water Research Institute and the Technion VPR Fund is gratefully acknowledged.

REFERENCES

1. Barby, D.; Haq, Z. Eur. Pat. 0,060,138, 1982.
2. Edwards, C. J.; Gregory, D. P.; Sharples, M. Eur. Pat. 87,302,517.5, 1987.
3. Elmes, A. R.; Hammond, K.; Sherrington, D. C. Eur. Pat. 88,303,675.8, 1988.
4. Williams, J. M. Langmuir 1988, 4, 44.
5. Williams, J. M.; Wroblewski, D. A. Langmuir 1988, 4, 656.
6. Cameron, N. R.; Sherrington, D. C. Colloid Polym Sci 1996, 274, 592.
7. Williams, J. M.; Gray, A. J.; Wilkerson, M. H. Langmuir 1990, 6, 437.
8. Kizling, J.; Kronberg, B. Colloid Surf 1990, 50, 131.
9. Aronson, M. P.; Petko, M. F. J Colloid Interface Sci 1993, 159, 134.
10. Hainey, P.; Huxham, I. M.; Rowatt, B.; Sherrington, D. C.; Tetley, L. Macromolecules 1991, 24, 117.
11. Guyot, A. Synthesis and Structure of Polymer Supports in Syntheses and Separations Using Functional Polymers; Sherrington, D. C.; Hodge, P., Eds.; Wiley: New York, 1988; Chapter 1.
12. Cameron, N. R.; Sherrington, D. C. Adv Pol Sci 1996, 126, 163.
13. Small, P. W.; Sherrington, D. C. J Chem Soc, Chem Commun 1989, 1589.
14. Schoo, H. F. M.; Challa, G.; Rowatt, B.; Sherrington, D. C. React Polym 1992, 16, 125.

15. Ruckenstein, E.; Hong, L. *Chem Mater* 1992, 4, 122.
16. Cameron, N. R.; Sherrington, D. C. *J Mater Chem* 1997, 7, 2209.
17. Tai, H.; Sergienko, A.; Silverstein, M. S. *Polymer* 2001, 42, 4473.
18. Tai, H.; Sergienko, A.; Silverstein, M. S. *Polym Eng Sci* 2001, 41, 1540.
19. Rehberg, C. E.; Fisher, C. H. *Ind Eng Chem* 1948, 40, 1429.
20. Fox, T. G. *Bull Am Phys Soc* 1956, 1, 123.
21. Nielsen, L. E.; Landel, R. F. *Mechanical Properties of Polymers and Composites*; Marcel Dekker, Inc.: New York, 1994; Chapter 7.
22. Brandrup, J.; Immergut, E. H.; Grulke, E. A. *Polymer Handbook*; John Wiley and Sons, Inc.: New York, 1999; Chapter 7.
23. Pouchert, C. J. *The Aldrich Library of FT-IR Spectra*; Aldrich Chemical Co.: Milwaukee, WI, 1985; Vol. 1.